

INDUSTRIAL AND ENGINEERING PAPER

Dual-band 3-way power divider and combiner based on CRLH-TLs

MOHAMMAD BEMANI AND SAEID NIKMEHR

In this paper, by using composite right and left handed transmission lines and non-radiating CRLH-TLs, a dual-band 3-way series power divider (SPD) is presented. The proposed dual-band divider is designed and fabricated on an inexpensive FR4 substrate of thickness $h = 0.79$ mm and a relative dielectric constant of $\epsilon_r = 4.4$ to work at 0.915 and 2.440 GHz. Also, in order to improve the isolation characteristics of this divider, three isolation resistors are implemented among output ports. Derived formulas are presented in details. The dual-band nature of the designed SPD, good input return loss, as well as equal power split among the three output ports, flexibility of spacing the output ports arbitrarily apart, and easy integration with planar devices make the proposed divider well suited for feeding many dual-band microwave circuits, such as multipliers, mixers, and planar array antennas. In addition, due to its excellent return-loss at the output ports and its high isolation, the proposed divider in this paper can be used as a power combiner.

Keywords: Dual-band, Series power divider (SPD), Power combiner, Composite right and left handed transmission line (CRLH-TL), Non-radiating CRLH-TLs (NR-CRLH-TLs), Isolation

Received 26 February 2015; Revised 19 April 2015; Accepted 23 April 2015; first published online 11 June 2015

I. INTRODUCTION

During the last years, due to requirement of dual-band and multi-band wireless communication systems, the researches on dual-band and multi-band components become very popular [1–4]. One of these components are dual-band N-way power dividers because they need to be connected to dual-band or multi-band antennas [5, 6]. In [7], based on the bagly polygon technique, a 4-way power divider was presented. Also, in [8, 9], multi-conductor lines were applied in order to design a 3-way and 4-way power dividers, respectively. But, the discussed dividers in [7–9] work only in a single frequency band.

By the way, composite right and left handed transmission lines (CRLH-TLs) and extended CRLH-TLs (E-CRLH-TLs) are one of the main developments in the field of metamaterials. The behavior of these materials; i.e. $\epsilon < 0$ and $\mu < 0$, has been used to design various multi-band component [10–15]. Recently, the CRLH-TLs were used to design a dual-band 4-way Wilkinson power divider in a parallel configuration. However, the performance of the divider reported in [16] is not good enough in terms of circuit size, and isolation because there is no isolation resistor between the output ports in this divider. By using series feed topology rather than parallel feed topology, the binary-tree transmission lines can be converted into a single feed line and consequently reducing significantly the overall dimension of the

structure [17]. In fact, series power dividers (SPDs) are usually used over parallel dividers in applications where power needs to be equally divided to a large number of loading elements and where the physical area of the feed network is limited. In [17] (Chapter 4), zero-degree metamaterial phase-shifting was used to design a 4-way SPD, but the operation of this divider is limited around a single frequency. Also, two drawbacks of the presented divider are their low isolation and their low output return losses. Therefore, these SPDs would not function well as a power combiner and they are not recommended to use as a power combiner.

In this paper, based on the CRLH-TLs, a dual-band 3-way SPD was designed and fabricated in order to work at $f_1 = 0.915$ GHz (from 0.902 to 0.928 GHz) and $f_2 = 2.440$ GHz (from 2.400 to 2.483 GHz). It is useful to note that the first frequency band is in the ultra-high frequency band and the second one is in the industrial scientific and medical band. The proposed divider provides equal and in-phase signals for three output ports. Also, isolation resistors are implemented among output ports to improve the isolation and output return loss characteristics of the designed divider. It should be emphasized that, in contrast to [17, 18], the proposed SPD in this paper can be used as a power combiner.

The organization of this article is as follows: Section II presents design methodology leading to dual-band CRLH-TLs and non-radiating CRLH-TL (NR-CRLH-TLs). Section III introduces a dual-band 3-way SPD and guideline for isolation and output return loss improvement. The simulated and the experimental results are discussed in Section IV. Finally, the conclusions are made in Section V.

Electrical and Computer Department, University of Tabriz, Tabriz, Iran

Corresponding author:

M. Bemani

Email: Bemani@tabrizu.ac.ir

II. THEORY: DUAL-BAND CRLH-TLS AND NR-CRLH-TLS

A) Analysis of CRLH-TLS

As we know, the non-linear phase response of CRLH-TLS can be engineered in order to produce desired phase shifts of ϕ_1 and ϕ_2 at two arbitrary frequencies of f_1 and f_2 , and design dual-band CRLH-TLS [19]. Therefore, Under balance condition, the required parameters for dual-band CRLH-TLS are given by [3]

$$d = \frac{\phi_1 f_1 - \phi_2 f_2}{2\pi n \sqrt{LC}(f_2^2 - f_1^2)}, \tag{1}$$

$$C_o = \frac{n(f_2^2 - f_1^2)}{2\pi Z_o(\phi_1 f_2 - \phi_2 f_1) f_1 f_2}, \tag{2}$$

$$L_o = \frac{nZ_o(f_2^2 - f_1^2)}{2\pi(\phi_1 f_2 - \phi_2 f_1) f_1 f_2}, \tag{3}$$

where d , Z_o , L , and C are the length, the characteristic impedance, the intrinsic inductance and the intrinsic capacitance per unit length of the right handed transmission line, respectively.

B) Analysis of NR-CRLH-TLS

As discussed in [20], any structure that support fast waves (the waves with superluminal phase velocity ($V_\phi > V_{Light} = c$)) are prone to radiate into free space. Therefore, in microwave applications, in order to design non-radiating transmission line, each unit cell of the line must be designed such that the phase velocity of the line is less than that of light. This property can be achieved when the propagation constant of the line is more than that of free space, i.e. ($\beta_{BL} > K_o$), because the phase velocity is defined as ($V_\phi = \omega/\beta$).

On the other hand, as we know, for 0° CRLH-TLS, the propagation constant of the line is equal to zero. Therefore, the transmission line will be superluminal and will tend to radiate into free space [3]. In order to solve this problem the new topology which is known as NR-CRLH-TL has been proposed in [17]. The proposed transmission line has a phase velocity that is slower than the speed of the light and so will not prone to radiate. NR-CRLH-TLS is consisted of a conventional CRLH-TL and a conventional transmission line (C-TL) (as shown in Fig. 1). CRLH-TL must be designed such that the unit cell operates as non-radiating transmission line while the C-TL is inherently non-radiating. The phase response of NR-CRLH-TL is given by [17]

$$\begin{aligned} \Phi_{NR-CRLH-TL} &= \phi_{CRLH-TL} + \phi_{C-TL} \\ &= n \left(-\omega \sqrt{LC}d + \frac{1}{\omega \sqrt{L_o C_o}} \right) - \omega \sqrt{LC}d_{C-TL}. \end{aligned} \tag{4}$$

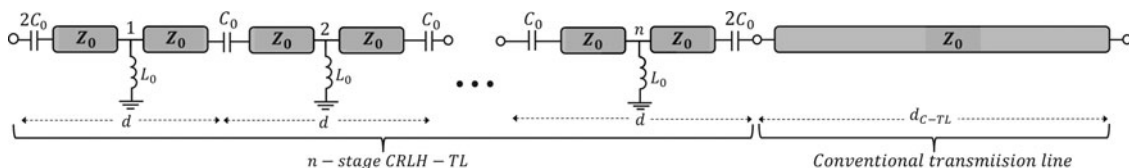


Fig. 1. Topology of n -stage NR-CRLH-TL [17].

Similar to CRLH-TLS the non-linear phase response of NR-CRLH-TLS can be controlled in order to design dual-band NR-CRLH-TLS. Therefore, the required parameters for dual-band NR-CRLH-TLS are given by [18]

$$d = \frac{(\phi_1 f_1 - \phi_2 f_2) f_1 + \phi_{C-TL}(f_2^2 - f_1^2)}{2\pi n \sqrt{LC} f_1 (f_2^2 - f_1^2)}, \tag{5}$$

$$L_o = \frac{nZ_o(f_2^2 - f_1^2)}{2\pi(\phi_1 f_2 - \phi_2 f_1) f_1 f_2}, \tag{6}$$

$$C_o = \frac{n(f_2^2 - f_1^2)}{2\pi Z_o(\phi_1 f_2 - \phi_2 f_1) f_1 f_2}, \tag{7}$$

where ϕ_{C-TL} is the phase shift of conventional transmission line and can be written as

$$\phi_{C-TL} = \phi_{C-TL} \Big|_{f_1} = \left(\frac{f_1}{f_2} \right) \phi_{C-TL} \Big|_{f_2}. \tag{8}$$

III. DUAL-BAND 3-WAY SPD

Fig. 2 displays the topology of the proposed dual-band 3-way SPD. As it can be seen in this figure, this divider consists of three types of CRLH-TLS as follows

- (I) Three dual-band $+90^\circ$ and -90° CRLH-TLS with characteristic impedance of $Z_o = 86.6 \Omega$ to provide a dual-band impedance transformation from the 50Ω test equipment impedance to the load impedance of 150Ω .
- (II) Three dual-band 0° and 180° NR-CRLH-TLS with characteristic impedance of $Z_o = 65.0 \Omega$ between the output ports in order to feed three 150Ω loads. Also, as discussed in [17] (Appendix B) that in order to achieve the maximum bandwidth for series power divider we need to use 0° (or 180°) transmission lines between output ports. Therefore, these loads are in parallel situation and resulting in a circuit with an input which is matched to 50Ω . Also, two dual-band 0° and 180° NR-CRLH-TLS are used at the end of the second and fourth ports in order to provide in-phase signals at the output ports.

Based on the design equations in Section II, the various dual-band CRLH-TLS and NR-CRLH-TLS in the structure of the proposed equal 3-way SPD were designed. Table 1 summarizes the values of the loading elements, the length and width of the RH-TLS and other characteristics of these lines.

A) Isolation study of 3-way SPD

As discussed in [21], the N-way divider or combiner can be matched at all ports, with good isolation between output

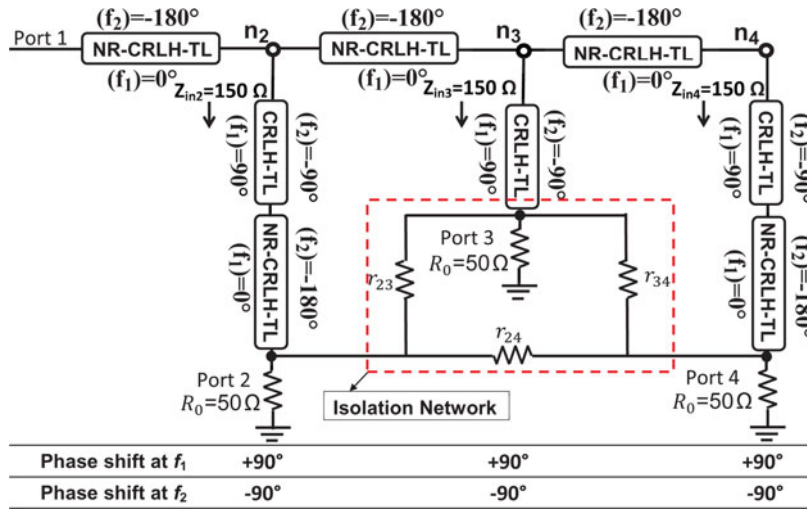


Fig. 2. Schematic diagram of the proposed dual-band 3-way SPD.

ports by using isolation resistors between all ports. Therefore, as shown in Fig. 3, three isolation resistors; i.e. r_{23} , r_{24} , and r_{34} are considered between output ports of the proposed 3-way SPD to improve isolation characteristics of this SPD. Since the NR-CRLH-TLs are of 0° and 180° at the two resonance frequencies, the joint of the three loads in Fig. 3, i.e. n_2 , n_3 , and n_4 , can be described as one node. The same simplification can be applied to the vertical NR-CRLH-TLs in Fig. 3. Thus, the proposed equal 3-way SPD can be modeled as a 4-port network circuit. Furthermore, in order to calculate the values of isolation resistors, an input signal is applied at one of the output ports (For example port 4) while port 1 is well matched. The above scenario is shown in Fig. 3.

Because of the symmetry in this figure, i.e. three equal output lines, we can assume that $r_{23} = r_{24} = r_{34} = r$. On the other hand, as is well known, the ideal isolation is obtained when the voltages of other output ports are zero. Regarding the Fig. 3, the transmission line voltages and currents giving rise to the following expressions [22]

$$V_1 = V_2 \cos \theta + j i_{20} Z_0 \sin \theta, \tag{9a}$$

$$i_{2i} = i_{20} \cos \theta + j V_{20} \sin \theta / Z_0, \tag{9b}$$

$$V_1 = V_3 \cos \theta + j i_{30} Z_0 \sin \theta, \tag{9c}$$

$$i_{3i} = i_{30} \cos \theta + j V_{30} \sin \theta / Z_0, \tag{9d}$$

$$V_1 = V_4 \cos \theta + j i_{40} Z_0 \sin \theta, \tag{9e}$$

$$i_{4i} = i_{40} \cos \theta + j V_{40} \sin \theta / Z_0. \tag{9f}$$

Also for the ports voltages we can write

$$V_1 = R_0 i_1 = 50 i_1, \tag{10a}$$

$$V_2 = R_0 i_2 = 50 i_2, \tag{10b}$$

$$V_3 = R_0 i_3 = 50 i_3, \tag{10c}$$

$$V_4 = V_5. \tag{10d}$$

And for the isolation resistors the Kirchoff's current law (KCL) equations are given by

$$V_2 - V_3 = r_{23} i_{23}, \tag{11a}$$

$$V_2 - V_4 = r_{24} i_{24}, \tag{11b}$$

$$V_3 - V_4 = r_{34} i_{34}. \tag{11c}$$

Finally, for five nodes, the KCL equations can be written as

$$i_1 + i_{2i} + i_{3i} + i_{4i} = 0, \tag{12a}$$

Table 1. Loading element values and pertinent characteristics of the two types of the dual-band line in Fig. 3 [18].

n		NR-CRLH-TL	CRLH-TL
		2	4
C_o (pF)	Calculated	3.90	3.13
	Available	3.30	3.30
$2C_o$ (pF)	Calculated	7.80	6.38
	Available	6.80	6.80
L_o (nH)	Calculated	16.49	23.97
	Available	18.00	22.00
d_{H-TL} (mm)	Calculated	8.34	6.71
	Adjusted	8.20	6.80
d_{C-TL} (mm)		23.00	0.00
W_{H-TL} (mm)		0.85	0.55

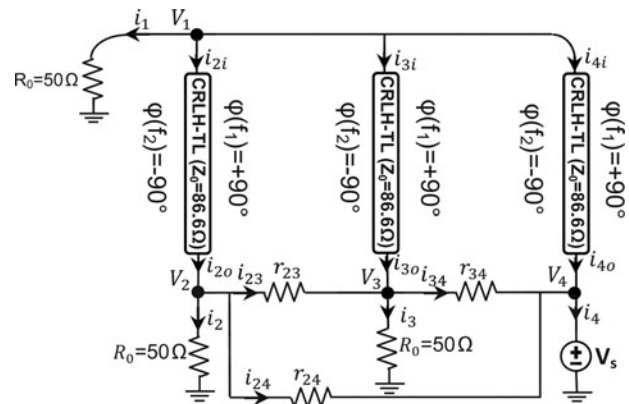


Fig. 3. The equivalent circuit of the proposed 3-way SPD (V_1, V_2, \dots and V_4 are the voltages of the nodes).

$$i_{20} = i_2 + i_{23} + i_{24}, \tag{12b}$$

$$i_{23} + i_{30} = i_3 + i_{34}, \tag{12c}$$

$$i_{24} + i_{34} + i_{40} = i_4. \tag{12d}$$

On the other hand, as is well known, the ideal isolation is obtained when the voltages of other output ports are zero. Therefore, a simple inspection of equations (9)–(12) with respect to the fact that $V_2 = V_3 = 0$ reveals that

$$r = \frac{Z_{\text{CRLH}}^2}{50} \Big|_{Z_{\text{CRLH}}=86.6} = 150 \Omega. \tag{13}$$

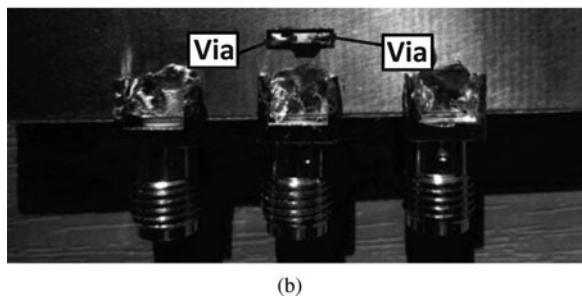
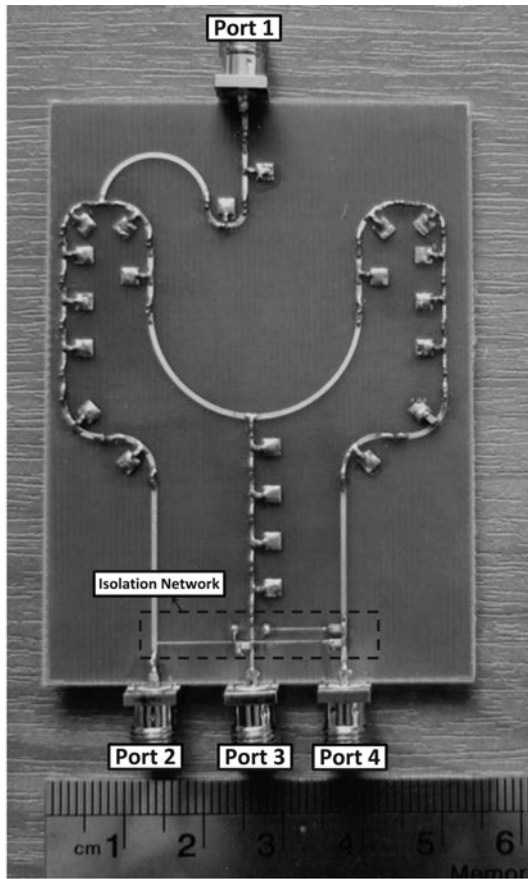


Fig. 4. (a) Fabricated prototype of the proposed dual-band 3-way SPD, (b) backside of the isolation network.

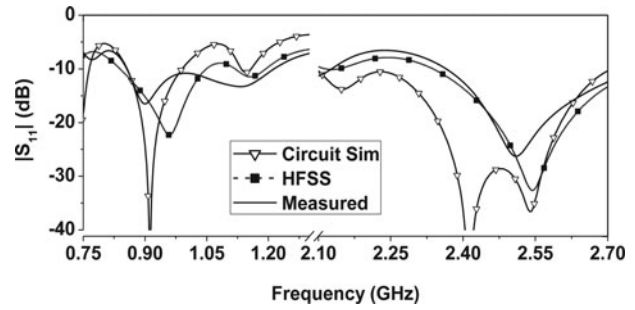


Fig. 5. Measured and simulated magnitude of S_{11} for the proposed dual-band 3-way SPD.

IV. SIMULATION AND EXPERIMENTAL RESULTS

The proposed 3-way SPD in this paper was designed and simulated using Agilent-ADS simulator. Also, in order to fully account parasitic and electromagnetic effects within the structure, full wave simulations were carried out in the high frequency structures simulator (HFSS) which is a full wave simulator based on the finite element method. Finally, the designed SPD was fabricated as shown in Fig. 4. It should be mentioned that in this paper, standard size of 0402 were used for the loading elements.

The presented results in this section are compared among the circuit, HFSS, and measured results. Fig. 5 shows the measured and the simulated magnitude of S_{11} for the proposed 3-way SPD. It should be mentioned that the small difference between measured and simulated results can be attributed to the small tolerance in substrate permittivity (FR4, $\epsilon_r = 4.4 \pm 0.1$) and non-ideal surface-mount technology (SMT)

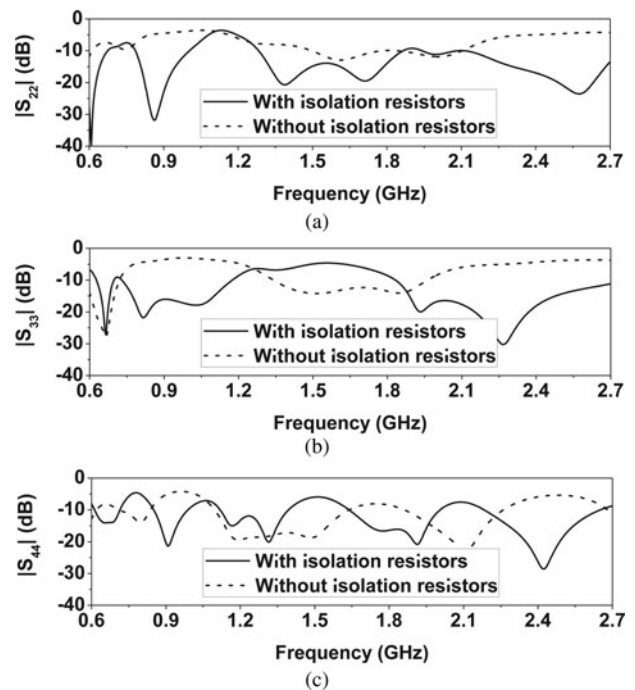


Fig. 6. Measured magnitude of (a) S_{22} , (b) S_{33} , and (c) S_{44} for the proposed dual-band 3-way SPD.

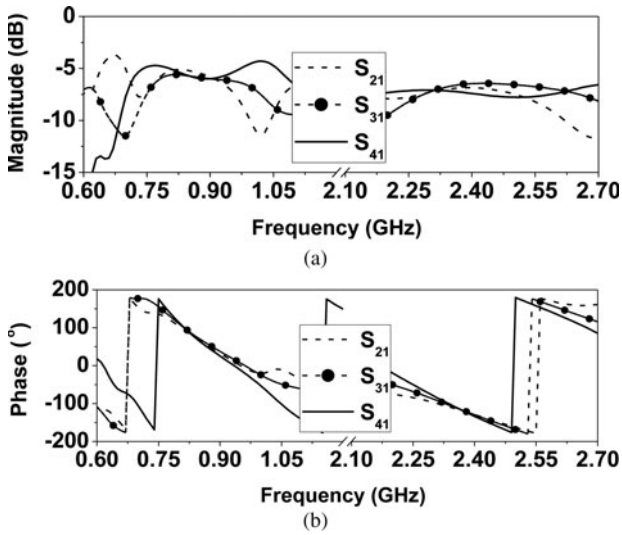


Fig. 7. Measured transmission characteristics to each of the output ports for the proposed dual-band 3-way SPD; (a) magnitude of S_{21} , S_{31} , and S_{41} , (b) insertion phase of S_{21} , S_{31} , and S_{41} .

component with value variation of $\pm 5\%$. As it can be seen, for the measured results the dual-band divider exhibits a measured -10 dB $|S_{11}|$ low frequency bandwidth of 0.36 GHz, from 0.85 to 1.21 GHz and a high frequency bandwidth of 0.41 GHz, from 2.36 to 2.77 GHz. In addition, the measured magnitude of S_{22} , S_{33} , and S_{44} for the proposed 3-way SPD are shown in Fig. 6. This figure exhibits the significant improvement of the output return losses after using the isolation resistors.

Also, Fig. 7 displays transmission characteristics to each of the output ports. It is obvious that the proposed dual-band divider provides equal and in-phase signals at output ports in the two passband. For demonstration, Fig. 8 shows the measured amplitude and phase balances of the proposed 3-way SPD which confirms that within the desired frequency bands, i.e. 0.902–0.928 GHz and 2.400–2.483 GHz, the measured amplitude and phase difference variations between output ports do not fluctuate beyond ± 0.5 dB and $\pm 10^\circ$,

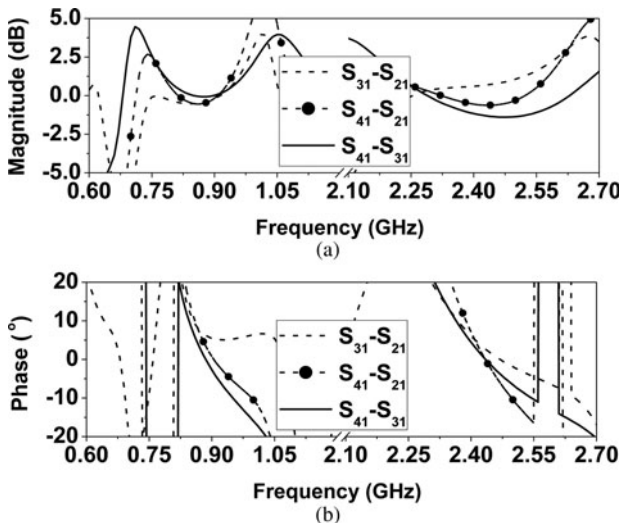


Fig. 8. (a) Amplitude and (b) phase balances of the proposed 3-way SPD.

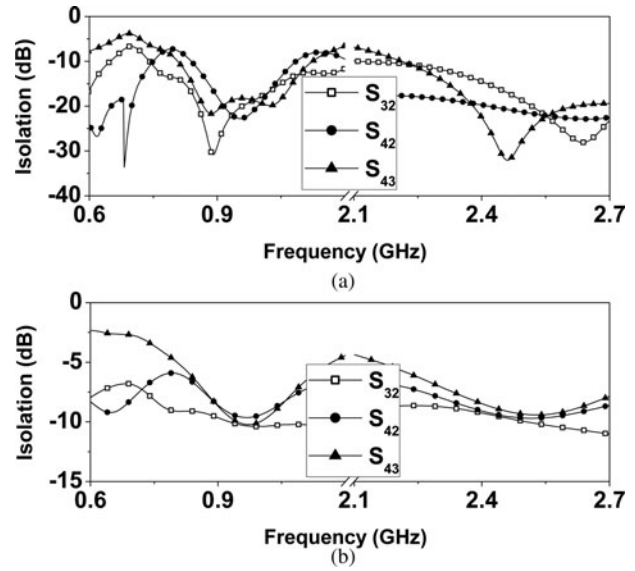


Fig. 9. Measured isolation between output ports of the proposed dual-band 3-way SPD; (a) with and (b) without isolation resistors.

respectively, from the values at 0.915 and 2.440 GHz. In addition, Fig. 9 depicts, the measured isolation characteristics between output ports of the designed 3-way SPD with and without isolation resistors. This figure confirms the significant improvement for this parameter after employing the isolation resistors. For detailed performance of this dual-band 3-way SPD, a summary is given in Table 2. It can be concluded that, due to excellent return-loss at the output ports and high isolation, the proposed SPD in this paper would function well as a power combiner and can be recommended to use as a power combiner. It should be noted that the extra losses in output ports can be attributed to non-ideal SMT component and the loss of the FR4 substrate. Also, more losses at

Table 2. Dimensions and measured performances of the 3-way SPD.

Operating frequency	0.915 GHz	2.440 GHz	
Circuit size (λ)	0.16×0.22	0.42×0.58	
Return loss (dB)	$ S_{11} $	15.84	16.71
	With isolation resistors $ S_{22} $	19.90	18.05
	$ S_{33} $	16.03	16.24
	$ S_{44} $	20.01	27.03
Insertion Loss (dB)	Without isolation resistors $ S_{11} $	18.34	18.82
	$ S_{22} $	4.74	5.49
	$ S_{33} $	3.35	4.11
	$ S_{44} $	4.74	5.49
Isolation (dB)	With isolation resistors $ S_{21} $	6.07	6.47
	$ S_{31} $	6.07	6.35
	$ S_{41} $	5.96	7.48
	Without isolation resistors $ S_{21} $	4.45	5.36
$ S_{31} $	5.50	5.88	
$ S_{41} $	5.82	6.20	
Isolation (dB)	With isolation resistors $ S_{32} $	25.26	16.11
	$ S_{42} $	19.77	20.43
	$ S_{43} $	19.86	29.51
	Without isolation resistors $ S_{32} $	9.91	9.54
$ S_{42} $	9.11	9.41	
$ S_{43} $	9.37	8.93	

2.44 GHz than in 0.915 GHz is from high dielectric loss in upper frequencies.

V. CONCLUSION

A dual-band non-radiating 3-way equal in-phase series power divider has been proposed in this paper. The proposed divider has been designed and implemented to work at 0.915 and 2.440 GHz. The designed divider exhibits good input return loss as well as equal power split to output ports in dual bands. Also, due to its excellent return-loss at the output ports and its high isolation, this type of power divider would function well as a power combiner. In addition, the dual-band nature of this divider, its compact size, low cost, ability to set the output ports arbitrary apart and easy integration with planar devices therefore renders it ideal for feeding many analog circuits, such as multipliers, mixers, amplifiers, and planar antenna arrays. The design concept of this paper can be easily extended to any number of output ports with arbitrary frequency and power dividing ratio.

ACKNOWLEDGEMENTS

This paper is published as part of a research project supported by the University of Tabriz Research Affairs Office. The authors are grateful to the University of Tabriz for financial supports.

REFERENCES

- [1] Zhang, H.-L.; Hu, B.-J.; Zhang, X.-Y.: Compact equal and unequal dual-frequency power divider based on composite right/left-handed transmission lines. *IEEE Trans. Ind. Electron.*, **59** (9) (2012), 3464–3472.
- [2] Kaura, J.; Khannaa, R.; Kartikeyan, M.: Novel dual-band multistrip monopole antenna with defected ground structure for WLAN/IMT/BLEETOOTH/WIMAX applications. *Int. J. Microw. Wireless Technol.*, **6** (1) (2014), 93–100.
- [3] Bemani, M.; Nikmehr, S.: Non-radiating arbitrary dual-band equal and unequal 1:4 series power dividers based on CRLH-TL structures. *IEEE Trans. Ind. Electron.*, **61** (3) (2014), 1223–1233.
- [4] Gence, A.; Baktur, R.; Jost, R.-j.: Dual-Bandpass filters with individually controllable passbands. *IEEE Trans. Compon. Packag. Manuf. Technol.*, **3** (1) (2013), 105–112.
- [5] Wong, K.L.: *Planar Antennas for Wireless Communications*, Wiley Inter-Science, Hoboken, NJ, 2003.
- [6] Anguera, J.; Andújar, A.; Huynh, M.C.; Orlenius, C.; Picher, C.; Puente, C.: Advances in antenna technology for wireless handheld devices. *Int. J. Antennas Propag.*, 2013 (2013), Article ID 838364, 1–25.
- [7] Shamaileh, K.-A.-A.; Qaroot, A.; Dib, N.: Design of N-way power divider similar to Bagley polygon divider with an even number of output ports. *Prog. Electromagn. Res. Lett. C.*, **20** (2011), 83–93.
- [8] Kim, S.; Jeon, S.; Jeong, J.: Compact three-way planar power divider using five-conductor coupled lines. *IEICE Electron. Express.*, **8** (17) (2011), 1387–1392.
- [9] Kim, S.; Jeon, S.; Jeong, J.: Compact two-way and four-way power dividers using multi-conductor coupled lines. *Microw. Wireless Compon.Lett.*, **21** (3) (2011), 130–132.
- [10] Rennings, A.; Otto, S.; Mosig, J.; Caloz, C.; Wolff, I.: Extended composite right/left-handed metamaterial and its application as quadband quarter-wavelength transmission line, in *Proc. Asia-Pacific Microw. Conf. (APMC)*, Yokohama, Japan, December 2006, 1405–1408.
- [11] Eleftheriades, G.V.: A generalized negative-refractive-index transmission-line (NRL-TL) metamaterial for dual-band and quad-band applications. *IEEE Microw. Wireless Compon. Lett.*, **17** (6) (2007), 415–417.
- [12] Bonache, J.; Sisó, G.; Gil, M.; Iniesta, A.; García-Rincón, J.; Martín, F.: Application of Composite Right/Left Handed (CRLH) Transmission Lines based on Complementary Split Ring Resonators (CSRRs) to the design of dual-band microwave components. *IEEE Microw. Wireless Compon. Lett.*, **18** (8) (2008), 524–526.
- [13] Papanastasiou, A.C.; Georghiou, G.E.; Eleftheriades, G.V.: A quad-band Wilkinson power divider using generalized NRI transmission lines. *IEEE Microw. Wireless Compon. Lett.*, **18** (8) (2008), 521–523.
- [14] Durán-Sindreu, M.; Vélez, A.; Aznar, F.; Sisó, G.; Bonache, J.; Martín, F.: Applications of open split ring resonators and open complementary split ring resonators to the synthesis of artificial transmission lines and microwave passive components. *IEEE Trans. Microw. Theory Tech.*, **57** (12) (2009), 3395–3403.
- [15] Durán-Sindreu, M.; Sisó, G.; Bonache, J.; Martín, F.: Planar multi-band microwave components based on the generalized composite right/left handed transmission line concept. *IEEE Trans. Microw. Theory Tech.*, **58** (12) (2010), 3882–3891.
- [16] Choi, J.-H.; Itoh, T.: Dual-band Composite Right/Left-Handed (CRLH) phased-array antenna. *IEEE Antennas Wireless Propag. Lett.*, **11** (2012), 732–735.
- [17] Antoniadis, M.-A.: *Microwave Devices and Antennas Based on Negative-Refractive-Index Transmission-Line Metamaterials*. Ph.D. thesis, University of Toronto, Toronto, ON, 2009.
- [18] Bemani, M.; Nikmehr, S.: Dual-band N-Way series power divider using CRLH-TL metamaterials with application in feeding dual-band linear broadside array antenna with reduced beam squinting. *IEEE Trans. Circuits Syst. I, Reg. Papers.*, **60** (12) (2013), 3239–3246.
- [19] Lin, I.H.; Vincentis, M.D.; Caloz, C.; Itoh, T.: Arbitrary Dual-Band component using right/left-handed transmission lines. *IEEE Trans. Microw. Theory Tech.*, **52** (4) (2004), 1142–1149.
- [20] Antoniadis, M.-A.; Eleftheriades, G.-V.: A broadband series power divider using zero-degree metamaterial phase-shifting lines. *Microw. Wireless Compon.Lett.*, **15** (11) (2005), 808–810.
- [21] Pozar, D.-M.: *Microwave Engineering*, 3rd ed., John Wily & Sons, Hoboken, NJ, 2005.
- [22] Cheng, D.-K.: *Field and Wave Electromagnetics*, 2nd ed., Addison-Wesley, New York, NY, 1989.



Mohammad Bemani received his B.S. degree in Electrical Engineering from the University of KN Toosi University of Technology, Tehran, Iran, in 2007, the M.S. and the Ph.D. degree from the University of Tabriz, Tabriz, Iran, in 2009 and 2013, respectively, in Electrical Engineering. From 2010 to 2013, he was a Teaching Assistant at the University of

Tabriz, where he contributed to the design and teaching of undergraduate courses relating to electromagnetics. During

the same period, he was a Research Assistant at the University of Tabriz, where he was involved in the development of microwave devices and antennas based on negative-refractive-index transmission-line (NRI-TL), metamaterials, and CRLH structures. His research interests include multi-band and UWB components, reconfigurable antenna, active circuits, dielectric resonator antennas, fractal antennas, composite right and left-handed structures, and negative-refractive-index transmission lines. He is currently an Assistant Professor in the Department of Electrical and Computer Engineering at the University of Tabriz, Tabriz, Iran.



Saeid Nikmehr Received his B.S. degree in Electrical Engineering from KN Toosi University of Technology, Tehran, Iran, and the M.S. and Ph.D. degrees, both from Syracuse University, Syracuse, NY, in 1988 and 1992, respectively. He is currently an Associate Professor in the Department of Electrical and Computer Engineering of University of Tabriz, Iran. His research interests involve microstrip antennas, microwave components design, and computational electromagnetics.